Modular Multilevel Converter Based Advanced Traction Power Transmission Substation for High Speed Railway Network in India

Venkatasupura Vemulapati[1], Y. N. Vijaykumar[2], N. Visali[3] and K. Kumar[4,*]

[1]*EEE Department, SASI Institute of Technology and Engineering, India*
[2]*Department of EEE, SVCET (A), Chittoor, India*
[3]*Department of EEE, JNTUA College of Engineering, Anantapur, India*
[4]*Department of EEE, Sri Venkateswara College of Engineering, Tirupati, India*
E-mail: vvsupura@svcolleges.edu.in; yn.vijaykumar@gmail.com; n.visali@gmail.com; kumar3kk@gmail.com
[*]*Corresponding Author*

Received 31 January 2022; Accepted 09 June 2022;
Publication 27 February 2023

Abstract

The current power transmission system for Indian railways facing difficulties with voltage unbalance, harmonics and circulation of negative sequence current throughout the power transmission line. In addition, the existence of neutral sections between two adjacent traction substations will cause the speed reduction and is considered as the main limitation for high speed. Traction load is a single phase in nature and it is very difficult to estimate the power flow from adjacent substations to locomotive as well as the location of the train. In this paper advanced common phase traction power transmission system is designed which is much appropriate for high speed railway (HSR) by eliminating neutral sections (NS) and overcome all the fore mentioned power quality (PQ) issues. A simplex algorithm is proposed to estimate the

Distributed Generation & Alternative Energy Journal, Vol. 38_3, 965–986.
doi: 10.13052/dgaej2156-3306.38311
© 2023 River Publishers

power flow and location of the train. The simulation results are analysed and low scale prototype model is built to validate the simulation outcomes. The results obtained are satisfactory and indicates the system suitability for high speed railway network.

Keywords: Traction power transmission systems, power quality, Indian railways, parallel inverters, droop control method.

List of Notations and Abbreviations

HSR High Speed Railway
PQ Power Quality
NRP National Rail Plan
SS Sub Stations
RPC Railway Power Controllers
NS Neutral Section

1 Introduction

Railway transportation has grown in importance since its beginning. Transportation is currently vital for urban growth and there is a clear global need for transportation [1]. According to the National Rail Plan (NRP) for India – 2030 [2], electrical railways are safer, cleaner, and more efficient than diesel railways [3]. The plan is to build a future resilient railway system by 2030. The NRP aims to develop solutions based on both operational and commercial policy approaches to enhance rail freight modal share. The plan aims to enhance the modal share of railways in freight traffic to much more (up to 45%) than the previous and maintain it [4].

1.1 Different Traction Power Supply System (TPSS) Schemes

Unlike other power systems, traction power supply has its own structure and approaches to PQ issues [5]. In the literature several traction power supply topologies, their issues, and solutions are proposed by many scholars. Traction power supplies are classified based on their features [6]. The traction supplies can be organized by their structure. Following are two primary traction power structures: conventional and common phase traction supply systems [7]. Finally, they are compared to highlight the benefits and drawbacks of each method.

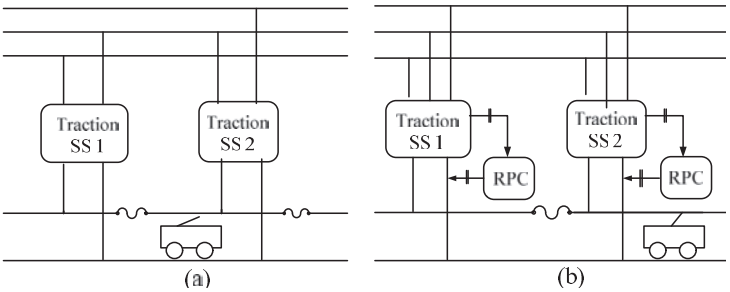

Figure 1 Traction power supply configurations (a) phase splitting method (b) combined phase method.

1.1.1 Conservative TPSS

Since traction motors run on single phase AC power, three phase electricity is normally split into two single phase outputs by traction transformers at substations (SS) [8]. As illustrated in the Figure 1(a). Supply lines between two successive substations and single phase outputs include NS to minimize the phase mixing [9]. This causes electrical separation between power zones. Power switching equipment is crucial when locomotives travel through these NS [10]. This reduces train power and speed. Excessive use of NS might result in power loss [11].

1.1.2 Combined phase TPSS

Recent proposals include combined phase TPSS to solve issues created by PQ and NS practices. Figure 1(b) depicts a typical power supply network with railway power controllers (RPC) [12]. Through a substation transformer, grid power is split into two single phase outputs and traction loads are coupled to the respective outputs, unlike typical traction power supplies. In this way, minimal phase mixing occurs, reducing the amount of NS needed [13]. In the event of a section power outage, eliminating physical separation aids a closed loop power supply system [14]. In fact, certain separators are isolated for maintenance purposes. There is some isolation need to be provided but not as much as usual. As a result, power loss owing to neutral sections or isolators can be minimized. Common phase traction power provides several benefits over traditional traction power in terms of design [15].

1.2 Power Quality of Traction Power Supplies

Locomotive loads are dynamic, time variable and nonlinear. As previously stated, it has the potential to cause a wide range of power quality issues

at the same time, including harmonic distortion [16]. The following are the major cases of traction power supply problems: Voltage unbalance and negative sequence currents; High reactive power and Harmonics are the important considerations. In reality, a number of distinct principles have been established for the PQ acceptance of diverse power systems. In this section, current challenges with traction power supply are discussed, along with the solutions that have been developed to address them. The IEEE and national standards are also cited as sources of information [17].

1.2.1 System unbalance and negative sequence currents (NSC)

Negative sequence and system unbalance are two of the utmost serious problems that can arise in traction power supply. It is possible for power systems to become unbalanced anytime if negative sequence components are present. It is possible that this is due to the connection of uneven loads [18]. Unbalance in the TPSS is produced by an imbalanced train load among the two phases of the system's operation. For long standing disturbances, the maximum voltage imbalance permitted at the grid connecting point is 2 percent [19], though for temporary disturbances, the maximum voltage unbalance allowed is 4 percent [20]. As an added bonus, this might be the industry standard for TPSS and balancing tolerance.

1.2.2 High reactive power

The reactive power in a power system is another source of concern for power quality [21]. When a load is capacitive or inductive, reactive power is pulled from power supply to compensate for this [22]. The high reactive power drawn from the power grid is a major cause of discomposure. It is the well-known power triangle, which depicts the combination of real and reactive components in terms of perceived power in a simple diagram. In addition, it must be remembered that the true power contribution used by system load is just the real power, and as a result, the quantity of reactive power spent should be kept to an absolute bare minimum [23].

1.2.3 Harmonics

In addition, the power oscillations and harmonics present a severe trouble in the TPSS. They are mostly referred to as the oscillating power that exists between the system supply and the system load. The use of nonlinear devices in the power system is expanding, and as a result, the harmonic problem is becoming more serious these days [24]. Because locomotives are nonlinear rectifier loads, this is an issue that also happens in the TPSS. The occurrence

of harmonics in a rotating machine can result in extreme losses, which can lead to machine failure. Harmonics in transformers can result in increased audible noise, copper losses, and magnetic losses. Traction power systems must thus have harmonic adjustment to function properly. The maximum individual frequency voltage harmonics for a traction system will be roughly 2 percent at the highest frequency [25].

2 Proposed Traction Substation Model for Indian Railways

The design described in this study is certainly a two way power design at the rectifier output, which comprises of three legs and each leg consists of six modules as indicated in Figure 2. A three phase MMC rectifier method

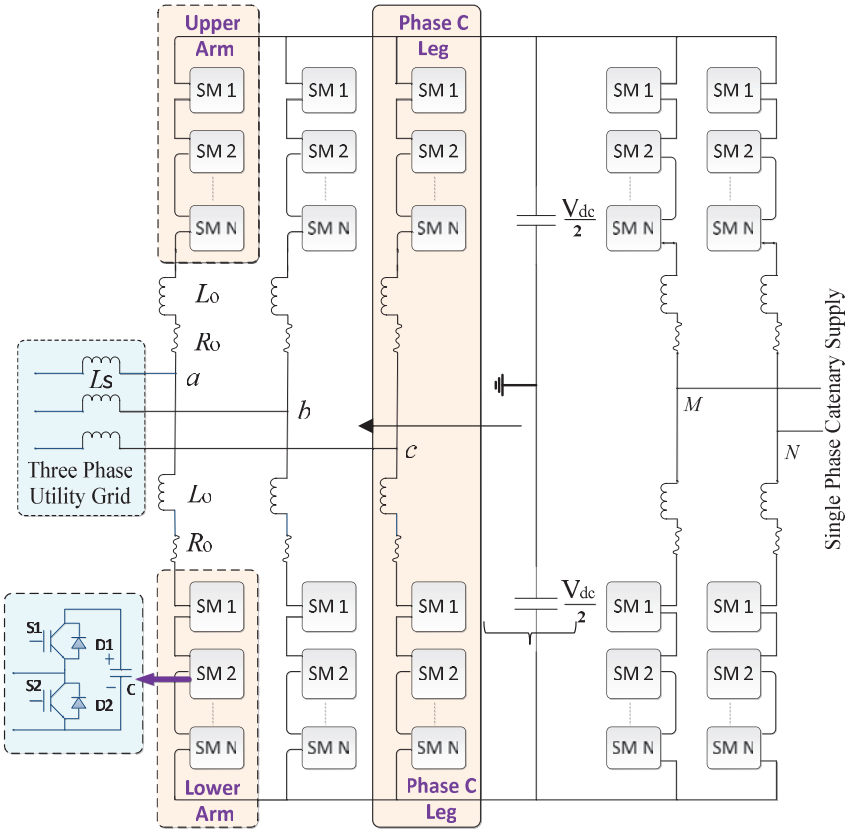

Figure 2 Proposed design of advanced traction substation.

and single phase inverter regulator structure are integrated in the whole MMC control system of the suggested alternative TPSS. The MMC rectifier controlling method includes of the DC voltage monitor and dual current loop control which preserve the stability of the DC voltage and ensure the working of the high power factor at the AC side. The single-phase MMC-based inverter in this work features a control methodology of cascaded control with droop control mechanism. The proposed traction power supply system's parameter is given here. The required RMS voltage at the single phase MMC output (V_{ac} rms) is 27.5 kV. The RMS to peak of the single MMC (Vac Peak) is $27.5\ \text{kV} * \sqrt{2} = 38.89$ kV. The Modulation Index selected as 0.7 (Maximum on time of each switch). As the MMC topologies are neutral point coupled, DC link voltage must be twice of the peak value of the AC required. Therefore, the required voltage at the MMC DC link bus (V_{dc}) is calculated as 80 kV. Now to obtain the above required DC link the rectifier output voltage can be calculated as 116.33 kV rms from the Equation (1), Output voltage of full bridge rectifier is as similar to DC link voltage ($V_o = V_{dc}$).

$$V_o = 0.955 V_{m,L-L} \tag{1}$$

Where, $V_{m,L-L}$ maximum line to line voltage. This is the peak value of the low voltage side of the transformer and in RMS $V_{rms,L-L} = 82.26$ kV. So as the AC grid is fixed at 132 kV the high voltage side is 132 kV in RMS. The capacitor is selected according to the MVA rating of traction substation and there a neutral point between so the capacitor is needed.

3 System Controlling

There are two parts of control present. One is decoupled 'dq' control for maintaining the DC link voltage as constant. The second one is a droop control for maintaining the single phase AC voltage. In the first example, the semiconductor switching losses are substantial. In these circumstances, the objective is to remove or considerably reduce low frequency harmonics to assist the processing of the AC voltage, because the kind of modulation employed controls, in part, the harmonics of the produced voltage. The voltage modulators as shown in Figure 3 are responsible for calculating the level of the output voltage at each sampling time, depending on the value of the AC voltage reference. When the number of converters levels is small, high-frequency modulation is often used, whereas when the number of levels is high, low-frequency steps are often used.

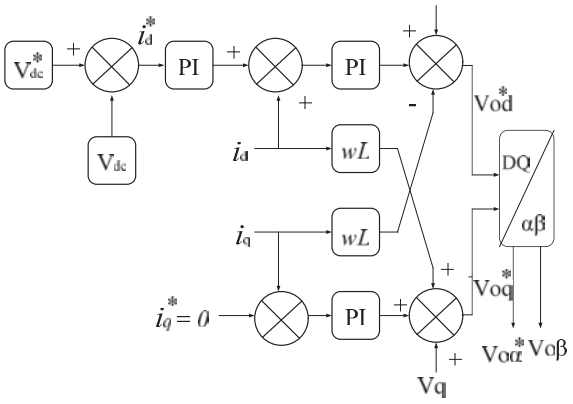

Figure 3 Voltage modulator DQ control.

Here there are two main Equations (2) & (3) are helpful to getting required I_d^* and V_{od}^*.

$$I_d^* = \left(k_p + \int k_i dt\right) \times (v_{dc}^* - v_{dc}) \tag{2}$$

$$V_{od}^* = \left(\left(k_p + \int k_i dt\right) \times (i_d^* + i_d)\right) - (i_q \times \omega L) + v_d \tag{3}$$

As the reactive power is not there in DC we can make $i_q^* = 0$ the equation can be written like

$$V_{oq}^* = \left(k_p + \int k_i dt\right) \times (-i_q) + (i_d \times \omega L) + v_q. \tag{4}$$

From v_α and v_β, V_A, V_B and V_C can be identified using the below Equations (5)–(9)

$$V_{s(\alpha)} = V_{s(pk)} \sin(\theta) \tag{5}$$

$$V_{s(\beta)} = V_{s(pk)} \cos(\theta) \tag{6}$$

$$v_A = \frac{2}{3} V_{s(\alpha)} \tag{7}$$

$$v_B = -\frac{1}{2} V_{s(\alpha)} + \frac{\sqrt{3}}{2} V_{s(\beta)} \tag{8}$$

$$v_C = -\frac{1}{2} V_{s(\alpha)} - \frac{\sqrt{3}}{2} V_{s(\beta)} \tag{9}$$

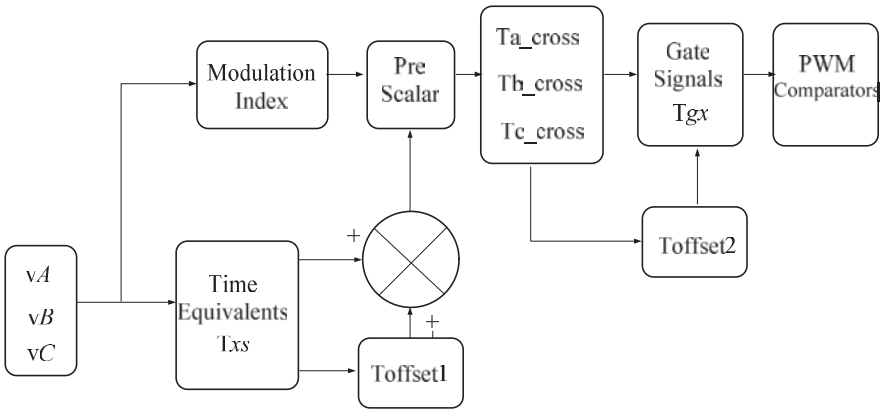

Figure 4 Time calculation and PWM generation in Multilevel SVPWM.

A multi-level PWM signal generating method derives the inverter exchanging times, from the measured reference phase voltage (V_A, V_B and V_C). The time circulation and PWM generation block is described in Figure 4. In this space vector PWM signal synthesis for any 'n'-level inverter, the time counterparts of the modulating signal (T_{as}, T_{bs}, T_{cs}) are combined with time offset $T_{offset1}$ to generate modified time equivalents of the voltage waveform $((T^*_{as}, T^*_{bs}, T^*_{cs}))$. The inclusion of $T_{offset1}$ to the reference voltage guarantees that the changed reference values always remain inside the carrier regions across the full iterative approach range.

$$T^*_{xs} = T_{xs} + T_{offset1}; \quad x = a, b, c \tag{10}$$

Where the magnitude of $T_{offset1}$ is as given earlier

$$T_{offset1} = -(T_{max} + T_{min})/2 \tag{11}$$

The adapted time counterparts of the reference voltage values are utilized to determine the time periods T_{across}, T_{bcross} and T_{ccross}.

The determination of T_{across}, T_{bcross} and T_{ccross}, when 'n' is odd, can be generalized as

$$T_{xcross} = T^*_{xs} + \{(I_x - (n-1)/2)T_s\}; \quad x = a, b, c \tag{12}$$

When 'n' is even, the determination of T_{across}, T_{bcross} and T_{ccross} can be generalized as [11].

$$T_{xcross} = T_s/2 + T_x s^* + (I_x - n/2)T_s; \quad x = a, b, c \tag{13}$$

Here I_a, I_b and I_c are the carrier indices for three phases. Then the time length for active exchanging vectors is cantered within the interval by adding an offset $T_{offset2}$ to T_{across}, T_{bcross} and T_{ccross}. Here the time offset $T_{offset2}$ is given as,

$$T_{offset2} = -\frac{\{\max(T_{x_{cross}}) + \min(T_{x_{cross}})\}}{2}; \quad x = a, b, c \tag{14}$$

The addition of time, $T_{offset2}$ to T_{across}, T_{bcross} and T_{ccross}, directly provides the inverter leg switching times T_{ga}, T_{gb} and T_{gc} for three phases.

$$T_{gx} = T_{xcross} + T_{offset2}; \quad x = a, b, c \tag{15}$$

The adapted time equivalents $(T^*_{as}, T^*_{bs}, T^*_{cs})$ have to be rescaled such that the improved signals are always within the carrier band. The T^*_{as}, T^*_{bs} and T^*_{cs} signals are appropriately clamped so that the basic component in the exclusive T^*_{as}, T^*_{bs} and T^*_{cs} the revised signal are the same and the adapted signal is always confined within the carrier section. Additionally, linear transfer attributes may be enlarged across the excessive modulation section up to six-step mode to obtain the highest utilization of DC link. The entire PWM signal production is performed just using the sampled frequency and amplitude of reference phase voltages and the methodology is exceptionally ideal for practical use on DSP control method.

4 Load Balancing at Inverter Side

In general, the location and amount of the traction load for load flow study are generally calculated by computing the efficiency of the locomotive relying on Newtonian laws of motion. Nevertheless, one such calculating technique may estimate the real power, which is actually utilised by the rail, but unable to forecast the reactive power. Additionally, the synchronized system data regarding the positions of all railroads within a particular section and total energy consumption of respective railroads are essential to correctly anticipate the operating states of several vehicles. Furthermore, such type of data is hard to quantify in realty, and getting the existing reporting data below the constant feeding condition is extraordinarily arduous.

4.1 Estimation of Load and Location Algorithm

MATLAB simulation is developed for analysing the standard feeding state of the equivalent traction load. Parallel posts that link the top and bottom

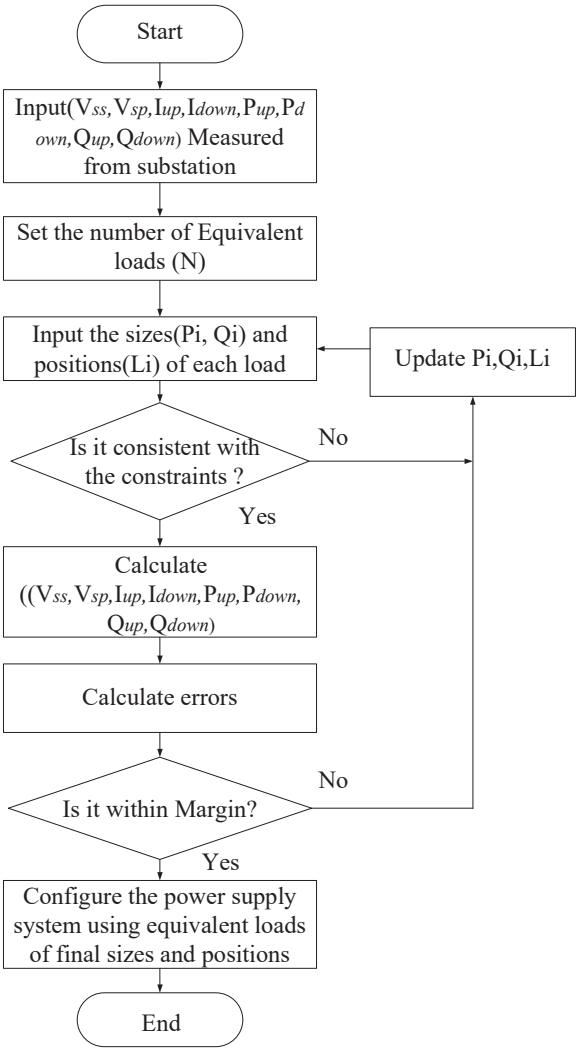

Figure 5 Estimation algorithm of load and location of the locomotive.

elements are usually installed across substation (SS) and section post (SP) to account for the power loss. Figure 5 illustrate the step-wise process for algorithm, which is used to estimate the load and location of locomotive. The objective function for the evaluation is represented by Equation (16). In addition, adequate weighting criteria were provided to permit the quick convergence of the findings. Each designed parameter can be calculated as

following:

$$\min_{P_iQ_iL_i} of(P_iQ_iL_i) = \omega_1\varepsilon_V + \omega_2\varepsilon_I + \omega_3\varepsilon_P \tag{16}$$

Where, ω_1, ω_2, and ω_3 are the weighting-factors and ε_V, ε_I and ε_P are the divergence errors. Equation (17) estimates the voltage prediction errors by correlating the voltages obtained at the real substation and section post with the simulator findings. For each sampling interval, the error is determined and expressed as follows:

$$\varepsilon_V = \int_{t_0}^{T} \{(V_{upw} - V_{upw_{ref}})^2 + (V_{dnw} - V_{dnw_{ref}})^2\}dt \tag{17}$$

Where V_{ss} and V_{sp} are the substation and section post voltages derived by the simulation and V_{ssref}, V_{spref} are the measured traction substation voltage magnitudes. Equation (18) Estimates the current forecast error by correlating the electrical impulses observed at the real SS with the reference simulated results as mentioned below:

$$\varepsilon_I = \int_{t_0}^{T} \{(I_{upw} - I_{upw_{ref}})^2 + (I_{dnw} - I_{dnw_{ref}})^2\}dt \tag{18}$$

Where, I_{upw}, I_{dnw} designed magnitudes of currents by the simulation, $I_{upw_{ref}}$, $I_{dnw_{ref}}$ reference currents at traction substation, Equation (19) is useful to compute the power approximation error by comparing the real and reactive powers measured at the real time SS and SP with the load flow investigation as extended as by the simulation, as follows:

$$\begin{aligned}\varepsilon_P = \int_{t_0}^{T} \{&(P_{upw} - P_{upw_{ref}})^2 + (P_{dnw} - P_{dnw_{ref}})^2 \\ &+ (Q_{upw} - Q_{upw_{ref}})^2 + (Q_{dnw} - Q_{dnw_{ref}})^2\}dt\end{aligned} \tag{19}$$

Where, $P_{upw}, P_{dnw}, Q_{upw}$ and Q_{dnw} magnitudes of real and reactive power designed by simulation; $P_{upw_{ref}}, P_{dnw_{ref}}, Q_{upw_{ref}}$, and $Q_{dnw_{ref}}$ magnitudes of reactive power at traction substation; (V_{SSref}, V_{SPref}) voltages measured at SS and SP; $P_{upw_{ref}}, P_{dnw_{ref}}$ reference real powers at traction substation; $Q_{upw_{ref}}, Q_{dnw_{ref}}$ reference reactive powers at traction substation.

Initially the measurement of reference parameters like voltage, current, real and reactive powers values $(V_{ss}, V_{sp}, I_{upw}, I_{dnw}, P_{upw}, P_{dnw}, Q_{upw}, Q_{dnw})$ at real time substation is essential. The algorithm will estimate the power consumption and location of the locomotives depends on the above

values. The TPSS is initially assumed approximately by setting the number of equivalent loads and respective locations. The designed simulated parameters $(V_{ss}, V_{sp}, I_{upw}, I_{dnw}, P_{upw}, P_{dnw}, Q_{upw}, Q_{dnw})$ are compared with the respective reference parameters $(V_{ssref}, V_{spref}, I_{upw}, I_{dnw}, P_{upw}, P_{dnw}, Q_{upw}, Q_{dnw})$ measured at the traction substation to calculate the errors. If the calculated errors are within the mentioned limits, the location and power of locomotives at that moment is found to be the final values and the algorithm is terminated.

5 MATLAB Simulation & Experimental Results

In this segment, simulation model and testing procedure has been applied to assess the system efficiency. All three models (i.e. three phase rectifier side control, DC link control and single phase Inverter side control) are simulated in the Simulink/ Matlab. The switching idea of the MMC is proven practically. As can be observed, the three control techniques comprising three phase rectification, DC link voltage and single phase inverter are together well. Three-phase utility grid voltage and current wave forms are shown in Figure 6, which shows that even the load fluctuations or it exchanges from substation to substation with high speed the variation is negligible. Figure 7 indicates the output voltage of synchronised parallel inverters of two successive traction substations with the application of droop control and Total Harmonic Distortion (THD) is also within the specified limit. The frequencies are compatible with all three control types as well. The circulation current will be dampened through the oscillating arm inductor and submodule capacitors. The quantity of peak current still relies on the configuration of the arm inductor and the capacitor for the MMC, but also fault diagnosis time. Important simulation parameters are listed in Table 1.

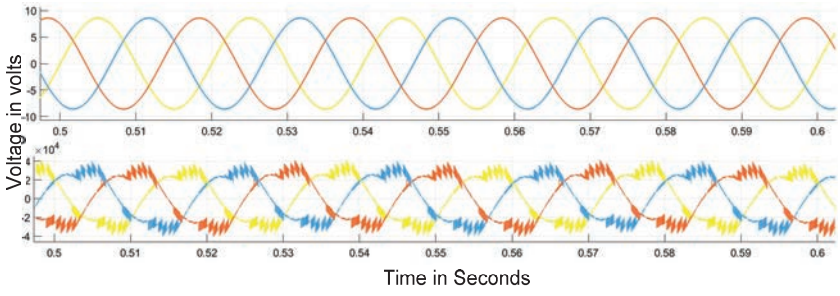

Figure 6 Three phase grid voltage and current waveforms.

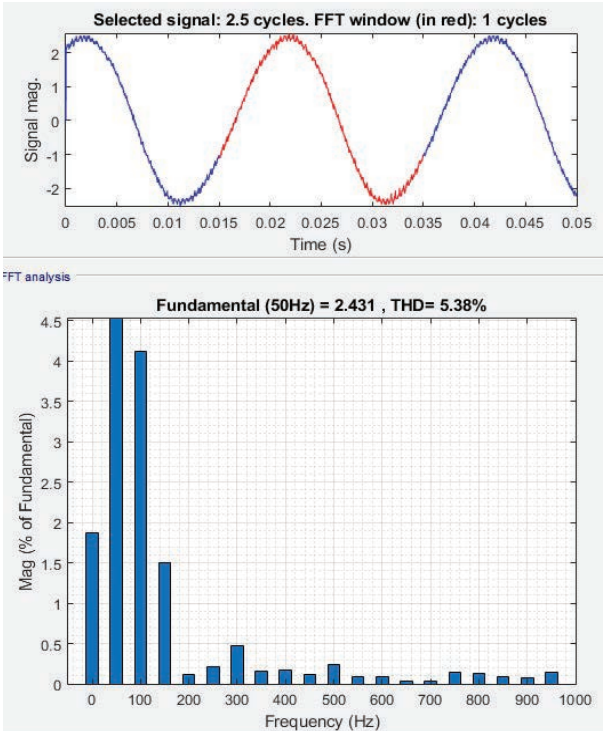

Figure 7 Single phase inverter output voltage waveform.

Table 1 Essential simulation parameters of the suggested scheme

Important Parameter	Value
Primary & Secondary voltage of transformer	132 kV/ 2850 V
DC Voltage reference value	5700 V
Switching frequency	1000 Hz
Capacity	35 MVA
Output voltage	27.5 kV

The designed magnitudes of SP & SS voltages and currents with respect to the simulation and actual measured values at traction substation under normal feeding traction substation is shown in Figure 8. The dotted line depicts the relative percentage error between both the measured and calculated values. The findings show that the predicted S/S and SP voltage, current, and power using the suggested technique and simplex estimations are very close to the measured values. DC-link voltages and all the module capacitor voltages are represented in Figure 9.

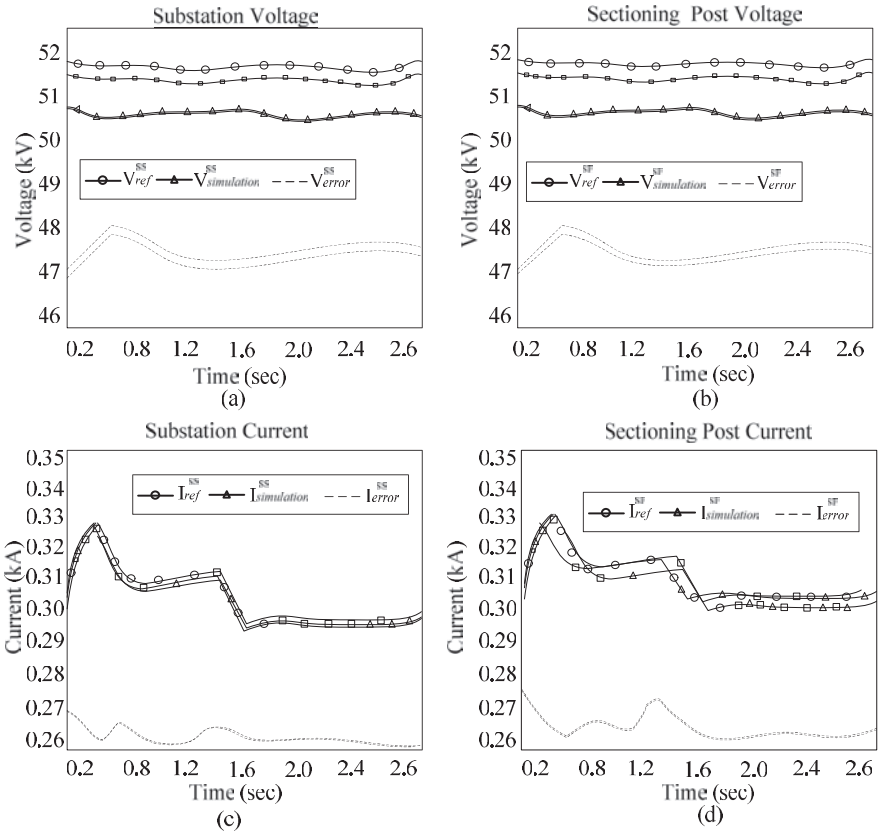

Figure 8 Simulation results under normal feeding condition (a) substation voltage current (b) sectioning post voltage (c) substation current (d) sectioning post current.

In order to conclude the study on MMCs with regard to modelling, control and design concerns, as well as the DC fault driving experience capacity of the MMC, the experimental activities should be undertaken. Experimental verification of the proposed analysis and methods for the MMC based traction substation is shown in Figure 10. The important experimental parameters are mentioned in the Table 2. Combined phase traction power supply system hardware setup testing to verify the operation of the back to back MMC converter is done.

Figure 11(a) depicts the three phase rectifier input side phase voltage waveform and FFT analysis is represented in Figure 11(b). The synchronized

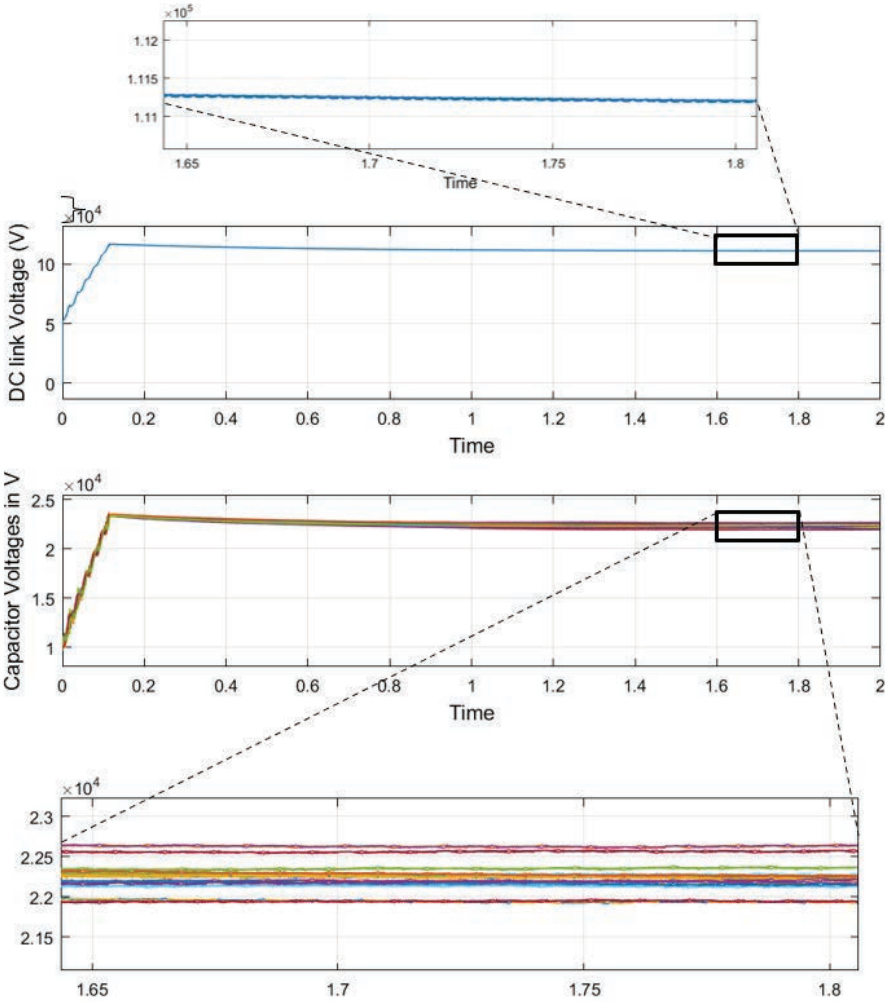

Figure 9 DC-link voltage waveform.

output voltage of two parallel single phase inverters without filter and with filter is shown in Figure 12(a) and 12(b) respectively.

The output voltages parameters of the three traction substations are similar in terms of phase, amplitude, and frequency, indicating that the proposed MMC-based traction power supply system described in this paper is capable of achieving the integral connectivity of the traction network.

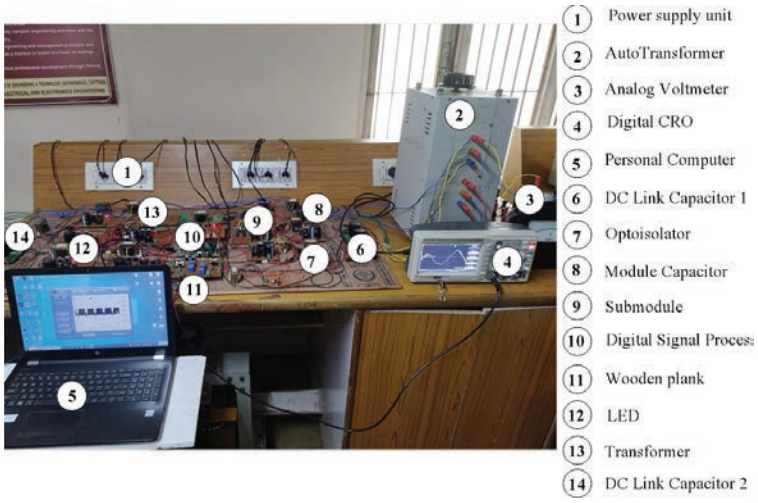

Figure 10 Experimental setup picture.

Table 2 Essential experimental parameters

Important Parameter	Value
Primary & Secondary voltage of transformer	110 V/ 90 V
DC Voltage reference value	230 V
Phase modulation inductance	0.9 mH
Output voltage	100V

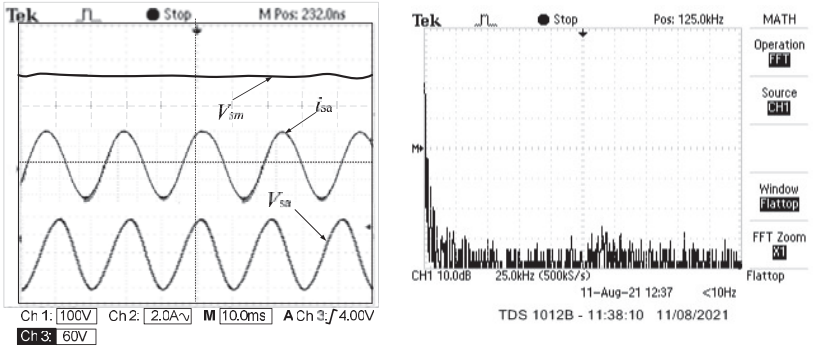

(a) (b)

Figure 11 Experimental results (a) waveforms of three phase rectifier in steady state. (Ch1: Submodule voltage V_{sm}, Ch2: AC-Side phase current i_{sa}, Ch3: AC-Side phase voltage V_{sa}) (b) FFT analysis of inverter.

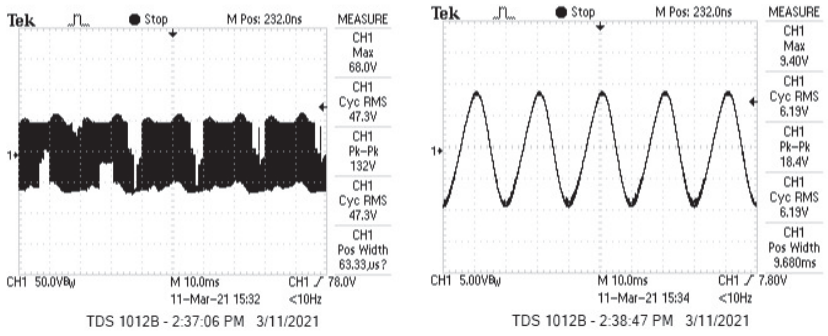

(a) (b)

Figure 12 Synchronised output voltage with droop characteristics (a) without filter (b) with filter.

6 Conclusion

In this article, modelling, control, and design consideration was conducted for the traction power supply system with the major attention on the high speed traction substation using the MMC with half bridge modules. The essential concepts of the development and control strategies of power converters including three phase MMC rectifier and single phase inverter through with DC link was explained. The mathematical approach for performance prediction of the converter was retrieved and the switching, averaging, and 'dq' model of the MMCs were established. Furthermore, the closed-loop control mechanism of the MMC and equilibrium of substation inverters were presented. An algorithm is created for the load balancing and estimation of locomotive position. The concept of the arm inductor and capacitor bank was addressed and the best switching frequency analysis of the MMCs was performed by examining the reliability of the converter.

References

[1] J. Zhang, J. Liu, S. Zhong, J. Yang, N. Zhao and T. Q. Zheng, "A Power Electronic Traction Transformer Configuration With Low-Voltage IGBTs for Onboard Traction Application," in IEEE Transactions on Power Electronics, vol. 34, no. 9, pp. 8453–8467, Sept. 2019, doi: 10.1109/TPEL.2018.2889107.

[2] Draft Final Report of the National Rail Plan-2030, Indian Railways, 2021.

[3] P. Cheng, H. Kong, J. Ma and L. Jia, "Overview of resilient traction power supply systems in railways with interconnected microgrid," in CSEE Journal of Power and Energy Systems, vol. 7, no. 5, pp. 1122–1132, Sept. 2021, doi: 10.17775/CSEEJPES.2020.02110.

[4] D. K. Saini, R. K. Nair C, B. V. Venkatasubramanian and M. Yadav, "Effect of Unaccounted Parameters on Reactive Power Compensation in Indian Electric Traction Line," in IEEE Access, vol. 8, pp. 182679–182692, 2020, doi: 10.1109/ACCESS.2020.3028582.

[5] D. Xiao, M. Chen and Y. Chen, "Negative sequence current and reactive power comprehensive compensation for freight railway considering the impact of DFIGs," in CPSS Transactions on Power Electronics and Applications, vol. 6, no. 3, pp. 235–241, Sept. 2021, doi: 10.24295/C PSSTPEA.2021.00022.

[6] X. He, J. Peng, P. Han, Z. Liu, S. Gao and P. Wang, "A Novel Advanced Traction Power Supply System Based on Modular Multilevel Converter," in IEEE Access, vol. 7, pp. 165018–165028, 2019, doi: 10.1109/ACCESS.2019.2949099.

[7] M. Li et al., "Four-Port Modular Multilevel AC/AC Converter in Continuous Co-phase Traction Power Supply Application," 2020 IEEE Energy Conversion Congress and Exposition (ECCE), 2020, pp. 1477–1481, doi: 10.1109/ECCE44975.2020.9236132.

[8] Y. N. Vijaykumar, V. Vemulapati, N. Visali, and K. Raju, "Railway Power Supply System using Modular Multilevel Converter with Droop Characteristics," 2020 4th International Conference on Electronics, Communication and Aerospace Technology (ICECA), Coimbatore, 2020, pp. 12–20, doi: 10.1109/ICECA49313.2020.9297599.

[9] Kumar, K., N. Ramesh Babu, and K. R. Prabhu. "Design and analysis of an integrated Cuk-SEPIC converter with MPPT for standalone wind/PV hybrid system." International Journal of Renewable Energy Research (IJRER) 7.1 (2017): 96–106.

[10] Krishnamurthy, Kumar, et al. "Power Electronic Converter Configurations Integration with Hybrid Energy Sources–A Comprehensive Review for State-of the-Art in Research." Electric Power Components and Systems 47.18 (2019): 1623–1650.

[11] W. Chou, A. Kempitiya and O. Vodyakho, "Reduction of Power Losses of SiC MOSFET Based Power Modules in Automotive Traction Inverter

Applications," 2018 IEEE Transportation Electrification Conference and Expo (ITEC), 2018, pp. 1035–1038, doi: 10.1109/ITEC.2018.8450130.

[12] M. Y. Artemenko, Y. V. Kutafin, V. M. Mykhalskyi, V. V. Chopyk, I. A. Shapoval and S. Y. Polishchuk, "The Control Strategy for Railway Power Conditioner in the Reference Frame of Two-Wattmeter Method," 2020 IEEE Problems of Automated Electrodrive. Theory and Practice (PAEP), 2020, pp. 1–4, doi: 10.1109/PAEP49887.2020.9240778.

[13] F. Ma et al., "A Railway Traction Power Conditioner Using Modular Multilevel Converter and Its Control Strategy for High-Speed Railway System," in IEEE Transactions on Transportation Electrification, vol. 2, no. 1, pp. 96–109, March 2016, doi: 10.1109/TTE.2016.2515164.

[14] H. Hayashiya et al., "Regenerative energy utilization in a.c. traction power supply system," 2016 IEEE International Power Electronics and Motion Control Conference (PEMC), 2016, pp. 1125–1130, doi: 10.1109/EPEPEMC.2016.7752152.

[15] V. Vemulapati, Y. N. Vijayakumar, and N. Visali, "Droop Characteristics based High Speed Traction Power Supply system using Modular Multilevel Converter," 2020 4th International Conference on Trends in Electronics and Informatics (ICOEI)(48184), Tirunelveli, India, 2020, pp. 111–118, doi: 10.1109/ICOEI48184.2020.9142920.

[16] V. Havryliuk, "Model of Propagation of Traction Current Harmonics from Trains to a Track Circuit Receiver," 2021 Asia-Pacific International Symposium on Electromagnetic Compatibility (APEMC), 2021, pp. 1–4, doi: 10.1109/APEMC49932.2021.9597152.

[17] "IEEE Standard for Power Electronics Open System Interfaces in Zonal Electrical Distribution Systems Rated Above 100 kW," in IEEE Std 1826–2020 (Revision of IEEE Std 1826–2012), vol., no., pp. 1–44, 25 Nov. 2020, doi: 10.1109/IEEESTD.2020.9271958.

[18] "IEEE Draft Recommended Practice for Design and Application of Power Electronics in Electrical Power Systems," in IEEE P1662/D8.0, March 2016, vol., no., pp. 1–63, 1 Jan. 2016, doi: 10.1109/IEEESTD.2016.7423638.

[19] "IEEE/IEC International Standard - Design and Verification of Low-Power Integrated Circuits," in IEC 61523–4 Edition 1.0 2015–03 (IEEE Std 1801–2013), vol., no., pp. 1–351, 24 March 2015, doi: 10.1109/IEEESTD.2015.7076554.

[20] "Historical Reliability Data for IEEE 3006 Standards: Power Systems Reliability," in 3006HistoricalData-2012 Historical Reliability Data for IEEE 3006 Standards, vol., no., pp. 1–303, 9 Nov. 2012, doi: 10.1109/IEEESTD.2012.6745993.

[21] Y. Danwen, L. Guanglei, W. Weixu and W. Qingyu, "Power quality pre-evaluation method considering the impact of electrified railway," 2021 6th Asia Conference on Power and Electrical Engineering (ACPEE), 2021, pp. 1556–1559, doi: 10.1109/ACPEE51499.2021.9436913.

[22] I. Nuca, V. Cazac, A. Turcanu and M. Burduniuc, "Development of Traction System with Six Phase Induction Motor for Urban Passenger Vehicle," 2020 International Conference and Exposition on Electrical And Power Engineering (EPE), 2020, pp. 749–754, doi: 10.1109/EPE50722.2020.9305555.

[23] T. Serdiuk, M. Feliziani and K. Serdiuk, "Research on Return Traction Current Harmonics," 2020 International Symposium on Electromagnetic Compatibility – EMC EUROPE, 2020, pp. 1–4, doi: 10.1109/EMCEUROPE48519.2020.9245808.

[24] H. Wang and J. Li, "Traction Network Resonance Suppression Strategy Based on Auxiliary Filter Winding of Traction Transformer," 2021 4th International Conference on Advanced Electronic Materials, Computers and Software Engineering (AEMCSE), 2021, pp. 249–252, doi: 10.1109/AEMCSE51986.2021.00059.

[25] P. -M. Nicolae et al., "Theoretical and Practical Aspects of Harmonics from a Railway Traction System Supplying Line," 2020 IEEE International Symposium on Electromagnetic Compatibility & Signal/Power Integrity (EMCSI), 2020, pp. 488–493, doi: 10.1109/EMCSI38923.2020.9191508.

Biographies

Venkatasupura Vemulapati received the Bachelor's degree in Electrical and Electronics Engineering from K L University (Formerly KL College of Engineering), Guntur, India in 2010 and a Master's degree in Electrical Power Systems from JNTUA College of Engineering, Ananthapur, India in 2012.

Presently he is pursuing doctoral degree in JNTUA College of Engineering, Ananthapur, India. His research interests include power converters and traction power supply networks for high speed railway.

Y. N. Vijaykumar received his Ph.D. in Electrical Engineering from JNTUA College of Engineering, Kakinada, India in 2016. He is currently working as a Professor & Head of the Electrical and Electronics Engineering department at Sri Venkateswara College of Engineering & Technology (A), Chittoor, India. His research interests include power electronic converters, control engineering and power quality analysis in power system.

N. Visali received Ph.D degree from JNTUA College of engineering, Ananthapur, India in 2013. She has a background in system Administration and presently she is working as a Professor in JNTUA College of Engineering, Ananthapur, India. She has published more than 50 research articles in leading journals, conference proceedings and books. Her research interests include Electrical distributing systems, FACTS devices and deregulated power systems.

K. Kumar is currently working as Associate professor in Dept. of EEE at SV College of Engineering (SVCE), Tirupathi, India. He received his Ph.D degree in 2019 from SELECT at VIT University, Vellore, India. M.Tech., degree in Power Electronics and Electrical Drives from the SV College of Engineering and Technology, Chittoor, JNTU-A, in 2013 and B.Tech., degree in Electrical and Electronics Engineering from the SV College of Engineering, Tirupathi, JNTU-A in 2011. His Research work focused in the field of power electronic applications in renewable energy sources and hybrid electric vehicles. He has published more than 25 research publications in various International Journals/Conferences. He is ratified as Assistant Professor from JNTU-A, ANANTHAPURAMU. He is a Permanent member of AMIE, MISTE and IAENG.